Sound & Vibration 2024, 59(1), 1756.
https://doi.org/10.59400/sv.v59i1.1756

Article

The three-dimensional aircraft-runway coupled vibration response based on double-layer plate for semi-rigid base

Shifu Liu[1,2], Jianming Ling[1,2], Weiyu Mao[1,2], Tianxin Hou[1,2,*]

[1] The Key Laboratory of Road and Traffic Engineering, Ministry of Education, Tongji University, Shanghai 201804, China
[2] The Key Laboratory of Infrastructure Durability and Operation Safety in Airfield of CAAC, Tongji University, Shanghai 201804, China
*** Corresponding author:** Tianxin Hou, 2131316@tongji.edu.cn

CITATION

Liu S, Ling J, Mao W, Hou T. The three-dimensional aircraft-runway coupled vibration response based on double-layer plate for semi-rigid base. Sound & Vibration. 2024; 59(1): 1756. https://doi.org/10.59400/sv.v59i1.1756

ARTICLE INFO

Received: 22 September 2024
Accepted: 14 October 2024
Available online: 21 October 2024

Abstract: As global aviation expands, airport infrastructure faces growing pressure to accommodate larger and heavier aircraft. A key challenge is managing the vibration interaction between aircraft and runway during takeoff, taxiing, and landing, which affects runway durability and aircraft safety. While most research focuses on the surface layer, the role of the semi-rigid base, commonly used in China, is often overlooked. This study addresses this by analyzing the semi-rigid base's role in three-dimensional aircraft-runway coupled vibrations. Taking into account the semi-rigid base layer and the subgrade shear stiffness, the study establishes a three-dimensional aircraft-pavement coupled model, using the measured roughness data from Shanghai Pudong International Airport as model input. The new explicit integration method is employed to solve the model. The study examines how structural parameters influence dynamic responses like load factors, strain, and displacement. Numerical simulations reveal that the support function of the semi-rigid base and the shear stiffness of the subgrade play a crucial role in improving runway stiffness and performance. The impact of aircraft taxiing speed is also significant. Specifically, increasing the base layer modulus from 1.50 GPa to 2.50 GPa results in a significant strain reduction (from 16.5 με to 12.8 με), and increasing the base thickness reduces strain by up to 17.8%. Moreover, enhancing the subgrade shear stiffness leads to improved resistance to deformation, further reducing strain and displacement. Additionally, as taxiing speed increases, the mean dynamic load coefficient decreases due to the lift generated by the aircraft, while strain fluctuations in the pavement increase. However, changes in pavement structure have minimal impact on aircraft center-of-gravity acceleration. This research provides critical insights for optimizing aircraft and runway design, enhancing safety, and extending runway lifespan through a coordinated focus on the surface layer, semi-rigid base layer, and subgrade with shear stiffness.

Keywords: aircraft-runway vibration; semi-rigid base; dynamic response; pavement design; runway safety

1. Introduction

As global aviation expands, airport infrastructure is increasingly strained to accommodate the growing number of aircraft takeoffs and landings. This surge in air traffic has raised the demand for more robust and stable airport runways, particularly as aircraft continue to grow in size and weight. A key factor affecting the longevity and safety of runways is the complex vibration interaction between aircraft and runways during critical phases, such as takeoff, taxiing, and landing [1]. Understanding the mechanisms of vibration response in the aircraft-runway system is essential not only for optimizing runway design and extending its service life but also for enhancing aircraft safety and improving passenger comfort [2]. However, coupled

vibrations between aircraft and runways present a multi-dimensional challenge influenced by several factors, including taxiing speed, surface roughness, and the physical characteristics of the runway. In China, nearly all runways are constructed with a semi-rigid base, and 95% of the surfaces are rigid, typically using cement concrete. This dual-layer structure provides exceptional strength and resistance to deformation. Despite its widespread use, the role of the semi-rigid base in vibration response is not yet fully understood.

Irregularities in the runway surface and taxiing speed are critical factors in the vibration response of the aircraft-runway system. Uneven surfaces can increase vibrations, potentially leading to structural degradation and higher dynamic loads on aircraft [3]. Additionally, higher taxiing speeds can significantly raise the stress and deformation of the runway [4]. Although many researchers have used simplified two-dimensional models to study this vibration interaction, these models fail to capture the full complexity of the system. For instance, Liu et al. [5] analyzed the response to random runway irregularities and found that both surface irregularities and speed significantly affect the aircraft's center of gravity acceleration and dynamic load coefficient. Li and Guo [6] used a two-degree-of-freedom model to examine the impact of foundation shear stiffness, concluding that unevenness plays a key role in dynamic response. Chen et al. [7] investigated nonlinear behaviors but overlooked important coupling effects due to simplifications in their model. These models, which do not account for the complexity of aircraft motion in three-dimensional space, particularly regarding pitch and roll, have limitations in evaluating the spatial impact of vibrations. As Liu et al. [8] demonstrated, three-dimensional models provide a more accurate assessment of runway unevenness and its effect on aircraft dynamics.

While semi-rigid bases are widely used, much of the research on aircraft-runway interaction focuses on the pavement surface layer and often neglects the influence of the base layer. For example, Sawant [9] simplified airport pavements to rigid or semi-rigid surfaces modeled with thick plate elements and represented the base layer as a spring-damping system. Kim et al. [10] highlighted that such models primarily focus on the surface layer's response to aircraft loads, overlooking the base layer's contribution to the overall structural performance. This oversimplification can lead to inaccurate predictions of the runway system's behavior, particularly under heavy aircraft loads and complex environmental conditions. Conversely, research in vehicle-highway systems has recognized the importance of semi-rigid bases and double-layer plate structures. Patil et al. [11], for instance, used a double-layer plate model to study the interaction between the base and surface layers, showing that factors such as base stiffness and thickness are crucial for pavement response, particularly on flexible foundations under dynamic loads. The double-layer model offers a more precise description of pavement dynamics, especially when considering factors like vehicle speed and load frequency [12]. Neglecting the base layer in such studies can lead to an underestimation of the structure's dynamic response. Therefore, it is vital to fully consider the semi-rigid base's role in the performance and dynamic behavior of runway structures.

This study seeks to address these gaps by thoroughly examining the role of the semi-rigid base in three-dimensional aircraft-runway coupled vibrations. Using a three-dimensional model based on the Pasternak foundation, this research considers

both the surface layer and the semi-rigid base. The model applies the fourth runway of Shanghai Pudong International Airport as a case study, with the B737 aircraft serving as the representative model. It explores how varying structural parameters and taxiing speeds influence the coupled vibrations in the aircraft-runway system. Key dynamic responses—including aircraft load factors, runway strain, and displacement—are evaluated, as they are critical to assessing the structural integrity of runways and ensuring the safety of aircraft during taxiing and landing. This model provides a valuable framework for dynamic analysis in runway design, offering insights that will help extend runway service life and improve aircraft safety.

2. Model of the runway double-layer plate structure considering semi-rigid base

The runway structure, composed of the surface and base layers, is simplified into a double-layer thin plate with continuous interlayers. The foundation is modeled using the Pasternak model, which accounts for compressive and shear characteristics. The dynamic model of the viscoelastic foundation is illustrated in **Figure 1**. Belabed et al. [13,14] use the finite element method to study functionally graded sandwich beams and bi-directional functionally graded beams. Attia et al. [15] and Lakhdar et al. [16] apply the finite element method to investigate thick laminated composite shells and porous bi-directional FGM sandwich shells. Hu et al. [17,18] introduced a new structure-preserving method to analyze the dynamic response of Space Manipulator Systems and to explore the vibrations in an axially moving cracked cantilever beam. However, the aircraft-runway coupled model is relatively complex. Considering computational complexity and efficiency, this paper adopts the method of modal superposition to solve the vibration differential equation of the runway.

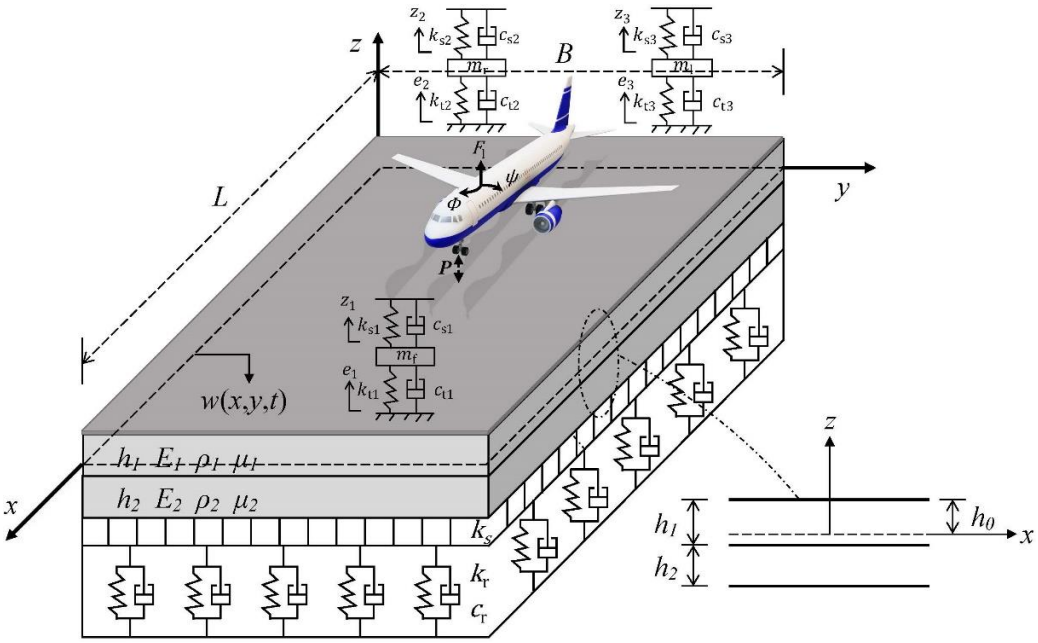

Figure 1. Dual-layer runway structure model.

In the model, P represents the force exerted on the runway by the aircraft wheel; $w(x, y, t)$ denotes the vertical displacement of the pavement structure; h_0 is the distance

from the neutral plane of the double-layer thin plate to the upper surface. The spatial coordinate system is established with the neutral plane as the *xy*-coordinate plane, where *x* and *y* correspond to the longitudinal and transverse directions of the runway, respectively, and the *z*-axis represents the depth direction, with the upward direction being positive. The variables h_1, E_1, ρ_1, μ_1 refer to the thickness, elastic modulus, density, and Poisson's ratio of the surface layer, respectively. Similarly, h_2, E_2, ρ_2, μ_2 denote the thickness, elastic modulus, density, and Poisson's ratio of the base layer. The parameters k_r, c_r, k_s correspond to the vertical stiffness, vertical damping, and horizontal shear stiffness of the foundation, respectively. The dimensions L and B represent the longitudinal length and transverse width of the pavement structure, with the surface and base layers sharing the same length and width.

The differential equation governing vibration is expressed as Equation (1).

$$D_s\left(\frac{\partial^4 w(x,y,t)}{\partial x^4}+\frac{\partial^4 w(x,y,t)}{\partial y^4}\right)+2\left(D_{xy}+2D_k\right)\frac{\partial^4 w(x,y,t)}{\partial x^2\,\partial y^2}+m_r\frac{\partial^2 w(x,y,t)}{\partial t^2}+k_r w(x,y,t)+c_r\frac{\partial w(x,y,t)}{\partial t}$$
$$-k_s\left(\frac{\partial^2 w(x,y,t)}{\partial x^2}+\frac{\partial^2 w(x,y,t)}{\partial y^2}\right)=\sum_{d=1}^{N_d}P_d(t)\,\delta(x-x_d)\delta(y-y_d) \tag{1}$$

where: N_d represents the number of aircraft wheel loads acting on the runway; P_d denotes the wheel load; $\delta(\cdot)$ is the Dirac delta function; x_d, y_d are the *x* and *y* coordinates of each wheel load, respectively. D_s, D_{xy} and D_k represent the flexural stiffness of the pavement structure.

Based on the method of modal superposition using a combination of bidirectional beam functions, the vertical displacement of the pavement structure can be represented as Equation (2).

$$w(x,y,t)=\sum_{m=1}^{NX}\sum_{n=1}^{NY}\Phi_{mn}(x,y)A_{mn}(t)=\sum_{m=1}^{NX}\sum_{n=1}^{NY}\sin\frac{m\pi x}{L}\sin\frac{n\pi y}{B}A_{mn}(t) \tag{2}$$

In the equations, *NX* and *NY* represent the cut-off modal orders in the *x* and *y* directions of the pavement structure, respectively. $A_{mn}(t)$ denotes the modal coordinate corresponding to the mode shape Φ_{mn}, which is a function of time *t*.

After rearranging, the second-order ordinary differential equation governing the vertical vibration of the runway is obtained as Equations (3) and (4).

$$\ddot{A}_{ij}(t)+\frac{c_r}{m_r}\dot{A}_{ij}(t)+\omega_{ij}^2 A_{\mathrm{mn}}(t)=\sum_{d=1}^{N_d}\frac{4}{LBm_r}P_d(t)\psi_i(x_d)\varphi_j(y_d) \tag{3}$$

$$\omega_{ij}^2=\frac{D_s\pi^4}{m_r}\left(\frac{i^4}{L^4}+\frac{j^4}{B^4}\right)+\frac{k_s\pi^2}{m_r}\left(\frac{i^2}{L^2}+\frac{j^2}{B^2}\right)+\frac{2\left(D_{xy}+2D_k\right)\pi^4}{m_r}\left(\frac{ij}{LB}\right)^2+\frac{k_r}{m_r} \tag{4}$$

3. Three-dimensional aircraft-runway coupling model

3.1. Aircraft model considering three-dimensional vibration

This study uses the B737 aircraft model as the research object because it is a representative example of a medium-sized passenger aircraft, widely used in global civil aviation. Its operational data can effectively reflect the dynamic response

characteristics of airport runways under typical operating conditions.

The detailed modeling of the aircraft is not included in this paper but refers to the model presented in previous studies [18]. In this paper, the three-dimensional vibrations of the aircraft are considered, including vertical vibration, pitch rotation, and roll rotation of the aircraft fuselage, as well as the vertical vibration of the three landing gears. These dynamic responses are crucial for accurately assessing the coupled vibrations between the aircraft and the runway system. This model effectively captures the essential degrees of freedom necessary to represent the aircraft's complex interaction with runway surfaces. Hu et al. [19] conducted a comprehensive study on the vibrational analysis of a finite plate when subjected to oblique impact. To simplify the model, this paper focuses on vertical impact.

The entire system of equations representing the aircraft's motion and dynamic response to runway roughness can be expressed concisely using Equation (5). This matrix-based approach allows for efficient computation and analysis of the coupled vibration behavior under various loading conditions and speeds.

$$[M_a]\{\ddot{X}_a\} + [C_a]\{\dot{X}_a\} + [K_a]\{X_a\} = \{P_{a2}\} \tag{5}$$

where, $[M_a]$ is the aircraft's mass matrix. $[C_a]$, $[K_a]$ is the damping matrix and the stiffness matrix. $\{X_a\}$ is the displacement of the aircraft. $\{P_a\}$ represents the external forces acting on the aircraft, mainly from runway interaction.

3.2. Aircraft and runway coupling

The coupling between the aircraft and the runway is reflected in the interaction between the aircraft wheels and the uneven runway surface. Uneven runway excitation leads to drastic changes in the displacement of the aircraft wheels, which in turn causes vibrations in the aircraft body. These vibrations are transmitted through the wheels to the runway, intensifying the dynamic load on the pavement. The resulting pavement displacement, combined with the unevenness of the surface, further excites the wheel vibrations. Therefore, the pavement excitation e experienced by each wheel consists of both the pavement displacement w and the unevenness q, which can be expressed by Equation (6).

$$e_d(t) = w_d(x_d, y_d, t) + q_d(x_d, y_d, t) \tag{6}$$

where, d represents the wheel number, and for a tricycle landing gear system with six degrees of freedom, the total number of wheels Nd is 3.

The pavement unevenness used in this study was obtained from the fourth runway of Shanghai Pudong International Airport. A three-dimensional laser point cloud static measurement was conducted, which is illustrated in **Figure 2**. Through multiple stitchings, the three-dimensional elevation of the runway was acquired, which is shown in **Figure 3**.

Figure 2. Three-dimensional laser point cloud static measurement.

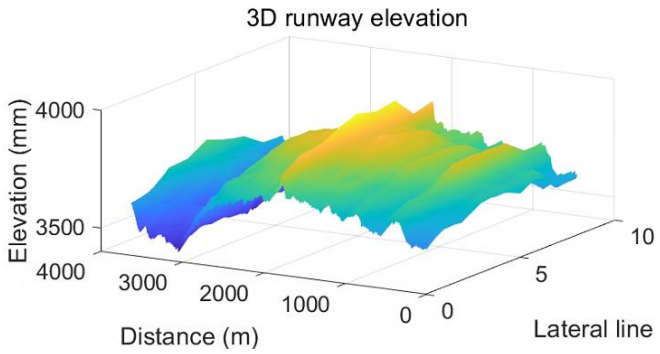

Figure 3. Three-dimensional elevation of the runway.

3.3. Aircraft-runway coupling model and equation

The dynamic interaction force between the aircraft and the runway excites vibrations in the aircraft upwards and induces vibrations in the runway downwards. This interaction force acts as a coupling mechanism that integrates the aircraft and runway sub-models into a unified model, varying in real-time according to the contact position of the aircraft wheel on the runway (**Figure 1**).

This interaction can be mathematically represented as Equation (7).

$$P_d(t) = k_d[z_d(t) - q_d(x_d, y_d, t)] - k_d \sum_{m=1}^{NX}\sum_{n=1}^{NY} \sin\frac{m\pi x_d}{L}\sin\frac{n\pi y_d}{B} A_{mn}(t) + c_d[\dot{z}_d(t) - \dot{q}_d(x_d, y_d, t)] - c_d \sum_{m=1}^{NX}\sum_{n=1}^{NY} \sin\frac{m\pi x_d}{L}\sin\frac{n\pi y_d}{B} \dot{A}_{mn}(t) - c_d \sum_{m=1}^{NX}\sum_{n=1}^{NY} \frac{m\pi V}{L}\cos\frac{m\pi x_d}{L}\sin\frac{n\pi y_d}{B} A_{mn}(t) \quad (7)$$

The dynamic contact between the aircraft wheels and the pavement occurs at multiple points, and during the runway taxiing process, the *x*- and *y*-coordinates of the aircraft wheels can be described by Equation (8).

For B737:

$$\begin{cases} x_1 = x_0 + Vt, & y_1 = y_0 \\ x_2 = x_0 - l_f - l_m + Vt, & y_2 = y_0 - b_r \\ x_3 = x_0 - l_f - l_m + Vt, & y_3 = y_0 + b_l \end{cases} \tag{8}$$

Therefore, the complete system of equations for the aircraft-runway system is obtained as shown as Equation (9).

$$\begin{cases} \ddot{A}_{ij}(t) + \dfrac{c_r}{m_r}\dot{A}_{ij}(t) + \omega_{ij}^2 A_{mn}(t) \\ = \dfrac{4}{LBm_r}\displaystyle\sum_{d=1}^{N_d}\Bigg[k_d(z_d - q_d) - k_d\sum_{m=1}^{NX}\sum_{n=1}^{NY}\sin\frac{m\pi x_d}{L}\sin\frac{n\pi y_d}{B}A_{mn}(t) + \\ c_d(\dot{z}_d - \dot{q}_d) - c_d\displaystyle\sum_{m=1}^{NX}\sum_{n=1}^{NY}\frac{m\pi V}{L}\cos\frac{m\pi x_d}{L}\sin\frac{n\pi y_d}{B}A_{mn}(t) - \\ c_d\displaystyle\sum_{m=1}^{NX}\sum_{n=1}^{NY}\sin\frac{m\pi x_d}{L}\sin\frac{n\pi y_d}{B}\dot{A}_{mn}(t)\Bigg]\sin\frac{i\pi x_d}{L}\sin\frac{j\pi y_d}{B} \\ [M_a]\{\ddot{X}_a\} + [C_a]\{\dot{X}_a\} + [K_a]\{X_a\} = \{P_{a2}\} \end{cases} \tag{9}$$

4. Model solution and verification

The aforementioned three-dimensional aircraft-runway coupling model is highly complex, particularly when the double-layer structure of the semi-rigid base is considered. This results in a high-degree-of-freedom, strongly coupled, and highly stochastic time-varying system. Due to these complexities, an appropriate numerical integration method is essential for solving the system. In this study, we introduce a novel explicit integration algorithm to address the computational challenges. Moreover, we demonstrate the accuracy and efficiency of this method for solving the aircraft-runway dynamic model.

This numerical method was initially developed for vehicle-track coupled dynamics. While this paper does not present any innovations related to the method itself, it is important to note that this is the first time the method has been applied to the aircraft-runway problem. The programming of the method has been successfully implemented in this study, and its accuracy and efficiency were compared and verified against the traditional Newmark-β method.

For the numerical simulations, a time step of 5×10^{-4} s was chosen, and all computations were performed on the same computer system. A comparison of the results obtained using two numerical integration methods is shown in **Table 1**. The variation curve of the aircraft's center of gravity acceleration is illustrated in **Figure 4**. The computation time for the two numerical integration methods is shown in **Figure 5**. It can be observed that the maximum deviation in dynamic responses, such as the center of gravity acceleration of the aircraft and pavement strain, is less than 0.01%, indicating that both methods yield identical computational accuracy. However, the computation time using the Newmark-β method is 1.85 times longer than that of the novel explicit integration method. This demonstrates that, under the same time step, the novel explicit integration method significantly accelerates the computation while maintaining equivalent accuracy. Therefore, the novel explicit integration method is

highly suitable for analyzing the aircraft-runway dynamic model.

Table 1. Comparison of the maximum response and calculation time obtained by two numerical integration methods.

Calculation Index	Newmark-β Method	New Explicit Integration Method	Relative Deviation (%)
Vertical Acceleration at Center of Gravity/(m/s2)	0.43940	0.43945	0.01096
Vertical Acceleration in Cockpit/(m/s2)	0.90565	0.90582	0.01885
Dynamic Load Coefficient of Front Landing Gear	1.14781	1.14781	0.00019
Dynamic Load Coefficient of Right Landing Gear	0.99483	0.99483	0.00002
Calculation Time/s	1114	601	185

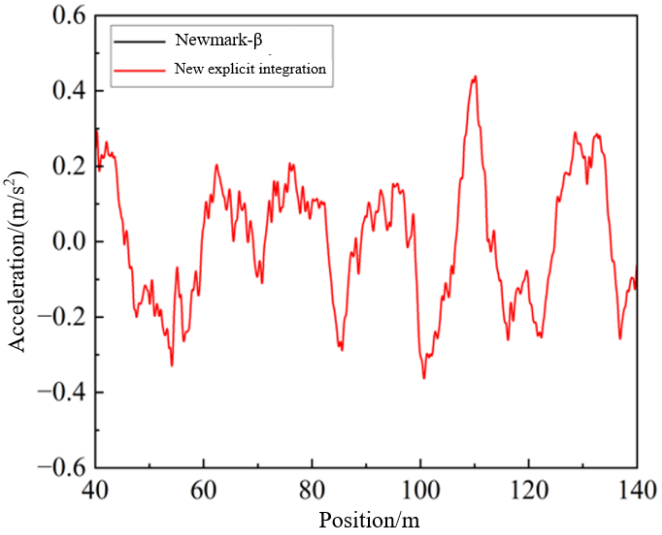

Figure 4. Variation curves of the aircraft's center of gravity acceleration.

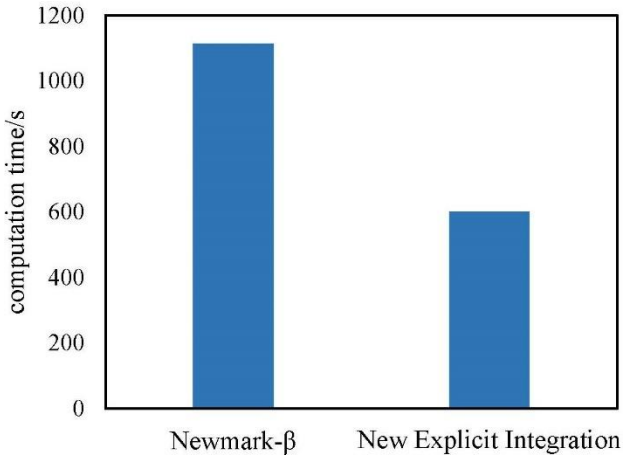

Figure 5. Computation time for two numerical integration methods.

5. Results and discussion

5.1. Effects of semi-rigid base thickness and modulus on structural response

This study is based on the Design Specification for Civil Airport Cement

Concrete Pavement (MH/T 5004-2019), which provides reference values commonly used in rigid pavements of Chinese airports. The surface layer thickness h_1 is set to 0.30 m, 0.34 m, 0.38 m, and 0.42 m, and the base layer thickness h_2 is set to 0.32 m, 0.36 m, 0.40 m, and 0.44 m, covering typical design values for Chinese rigid pavements. These values were selected to study the impact of different thickness combinations on the dynamic response of the pavement system. Additionally, the surface layer elastic modulus E_1 is set to 26, 30, 34, 38, and 42 GPa, and the base layer elastic modulus E_2 is set to 1.50, 1.75, 2.00, 2.25, and 2.50 GPa, to investigate the effects of different moduli on the pavement structure's strain and displacement. These parameter settings reflect typical material properties in airport pavements and provide a reliable foundation for studying the dynamic response of pavements under aircraft loads.

Numerical simulations reveal that variations in surface and base thicknesses and moduli significantly affect the strain and displacement of the pavement structure. As shown in **Figures 6** and **7**, when the surface layer thickness increases from 0.30 m to 0.42 m, the maximum strain decreases from 18.27 με to 16.17 με, a reduction of approximately 11.5%. At the same time, the maximum displacement decreases from 0.35 mm to 0.25 mm, a reduction of 28.6%. These changes demonstrate that increasing the surface layer thickness significantly improves the pavement's stiffness, reducing strain and displacement. As the base layer thickness increases from 0.32 m to 0.44 m, the maximum strain decreases from 19.35 με to 15.90 με, a reduction of 17.8%, while the maximum displacement decreases from 0.30 mm to 0.27 mm, a reduction of 10%. Although the impact of base thickness on displacement is smaller compared to surface thickness, the increase in base thickness has a significant effect on reducing strain, especially in areas of stress concentration.

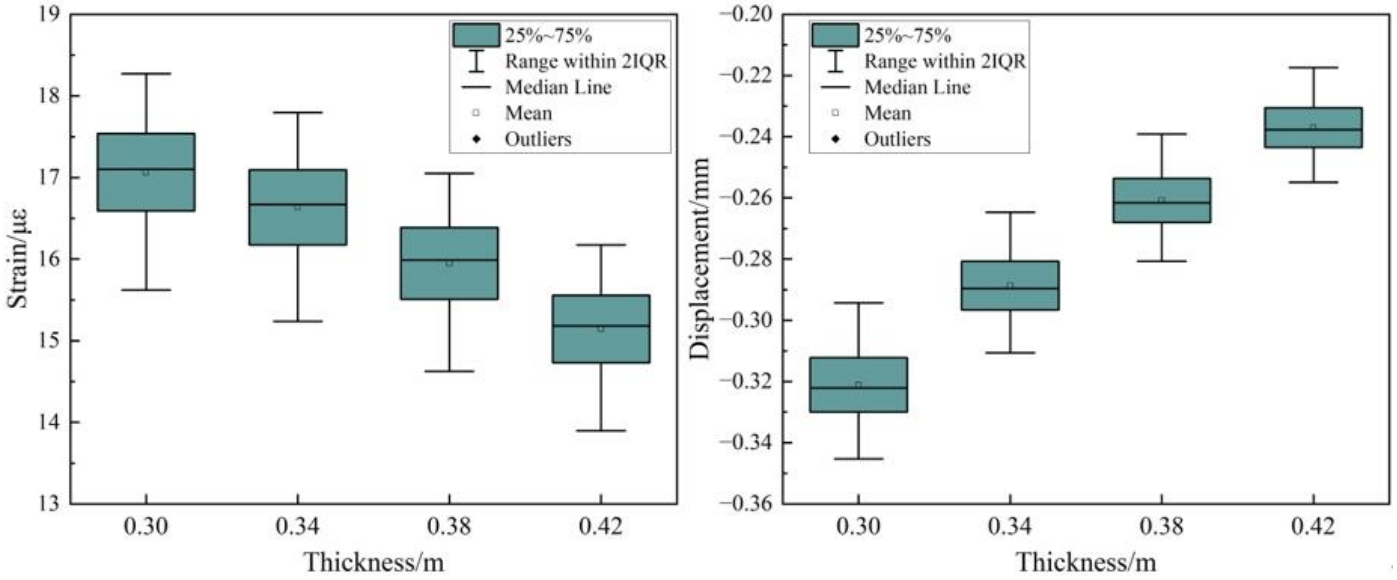

Figure 6. Dynamic response of pavement under different surface thickness.

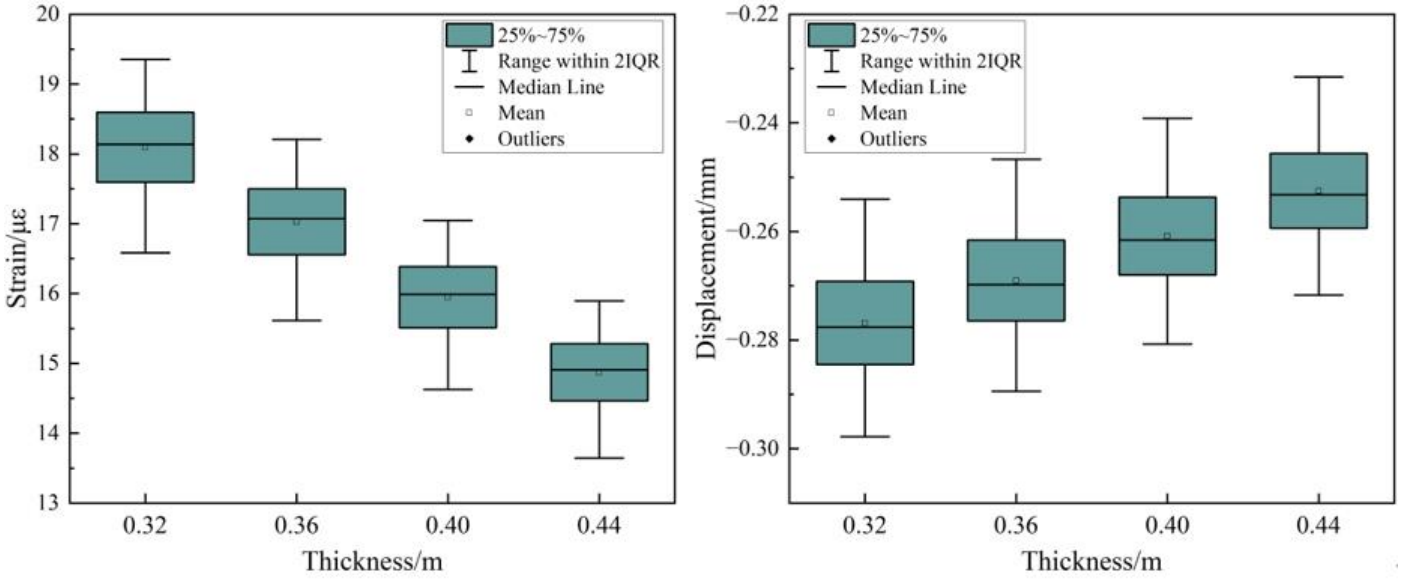

Figure 7. Dynamic response of pavement under different base thickness.

In terms of elastic modulus, increasing the surface layer modulus also significantly affects the pavement response. As shown in **Figures 8** and **9**, when the surface layer modulus increases from 26 GPa to 42 GPa, the maximum strain decreases from 18με to 14.8με, a reduction of approximately 17.7%, while the displacement decreases from −0.28 mm to −0.22 mm, a reduction of 21.4%. These results show that as the surface modulus increases, the stiffness of the surface layer improves, effectively controlling strain and displacement, and reducing surface deformation. The base layer modulus also plays a crucial role in controlling strain. As the base modulus increases from 1.50 GPa to 2.50 GPa, the maximum strain decreases from 16.5 με to 12.8 με, a reduction of 22.4%, and the displacement decreases from −0.28 mm to −0.23 mm, a reduction of 17.9%. This indicates that higher base moduli more effectively distribute stress, reducing internal strain and improving the structural stability of the pavement.

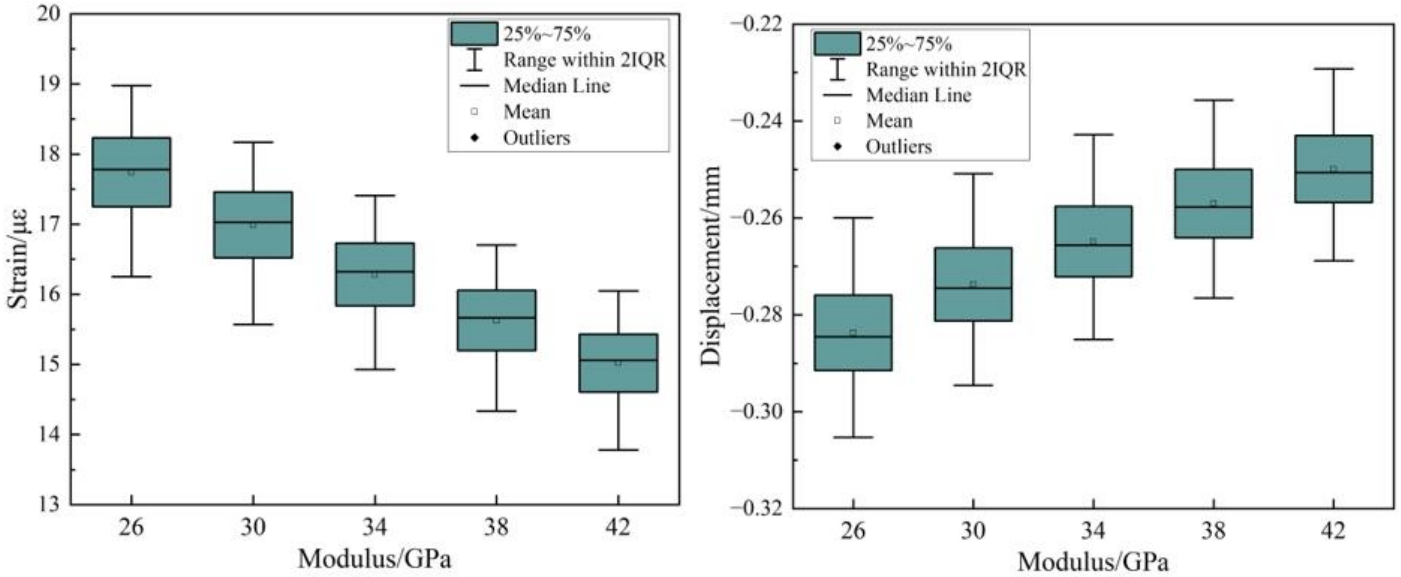

Figure 8. Dynamic response of pavement under different elastic modulus of surface layer.

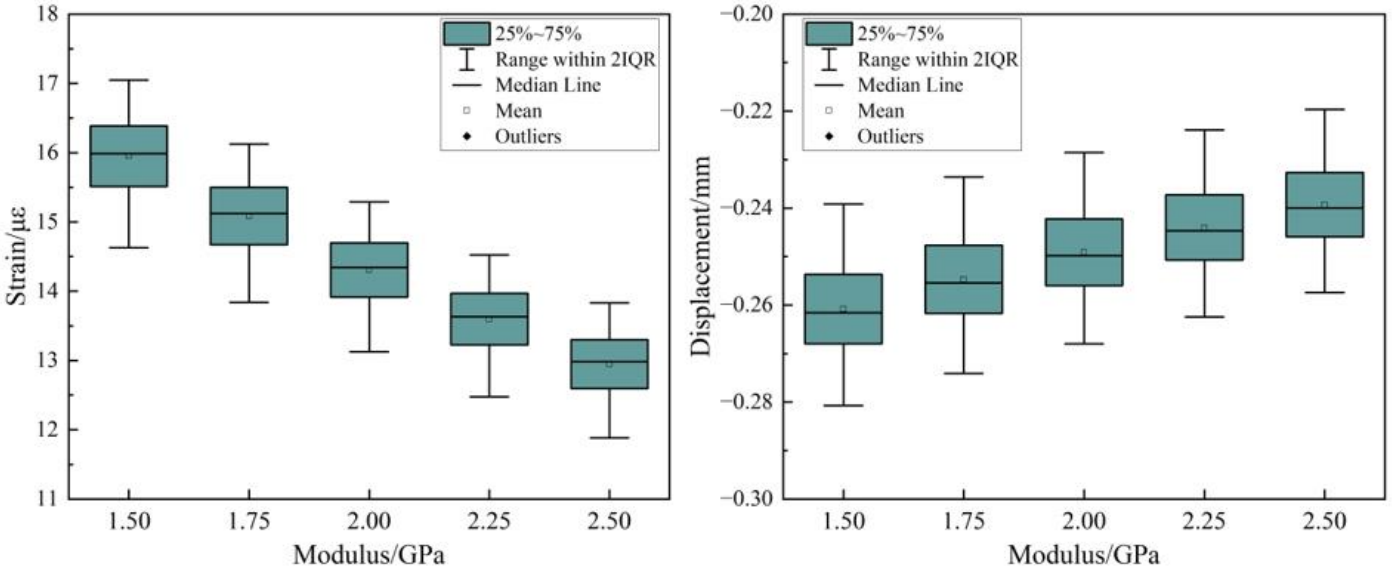

Figure 9. Dynamic response of pavement under different elastic modulus of base course.

These changes can be explained through stress transmission mechanisms. The increase in surface layer thickness and modulus enhances the pavement's resistance to deformation, significantly reducing displacement. However, this effect is dependent on the supporting role of the semi-rigid base. Increasing the base modulus effectively distributes the stress transferred from the surface layer, reducing stress concentration and significantly lowering strain within the pavement. This coordinated effect between surface and base layers is crucial in pavement design, ensuring optimal mechanical performance under long-term loads. Neglecting the design of the base layer's thickness and modulus could lead to stress concentration between the surface and base layers, increasing the risk of dynamic damage under uneven excitations from aircraft loads. Therefore, in runway design, a comprehensive consideration of both surface and base layer thicknesses and moduli is necessary to achieve the best structural performance and economic efficiency.

While the studies by Li et al. [20] and Sawant [9] focused on analyzing the dynamic response of the aircraft-pavement coupled system, particularly the effects of surface layer thickness and subgrade shear stiffness, they did not fully consider the role of the semi-rigid base layer. In contrast, this study is the first to investigate the significant impact of semi-rigid base thickness and modulus on pavement strain and displacement, demonstrating the critical role of the base layer in controlling the pavement structure's response. Furthermore, this study emphasizes the coordinated effect of surface and base layer thicknesses and moduli, highlighting the necessity of base layer design in optimizing pavement performance, thus offering new insights into the existing literature.

5.2. Impact of subgrade shear stiffness on structural response

This section investigates the impact of subgrade shear stiffness ks on the strain and displacement response of the pavement structure. Shear stiffness ks represents the ability of the subgrade material to resist shear deformation, and increasing this stiffness provides stronger lateral support to the pavement structure. In this study, the

shear stiffness values are set to 0, 40, and 100 MN/m, aimed at analyzing the effects of different shear stiffness levels on the dynamic response of the pavement system.

Firstly, from the strain variation graphs (**Figure 10**), it is observed that as the shear stiffness increases, the maximum strain in the pavement structure decreases significantly. When the shear stiffness ks increases from 0 MN/m to 100 MN/m, the maximum strain drops from nearly 17 με to about 13 με. In particular, in regions where strain fluctuates, higher shear stiffness helps to smooth out stress concentrations, significantly reducing strain response in the pavement. This demonstrates that the lateral shear stiffness of the subgrade effectively enhances the pavement's load-bearing capacity, dispersing external loads and reducing strain concentration, thereby improving the structural stability of the pavement. The boxplots (**Figure 11**) further confirm this trend, showing that with increasing shear stiffness, the median and interquartile range of strain both decrease, indicating better strain control.

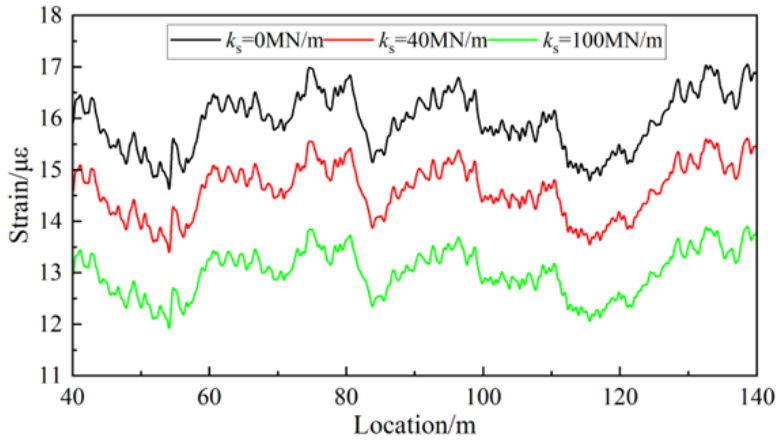

Figure 10. Dynamic strain of pavement under different shear stiffness.

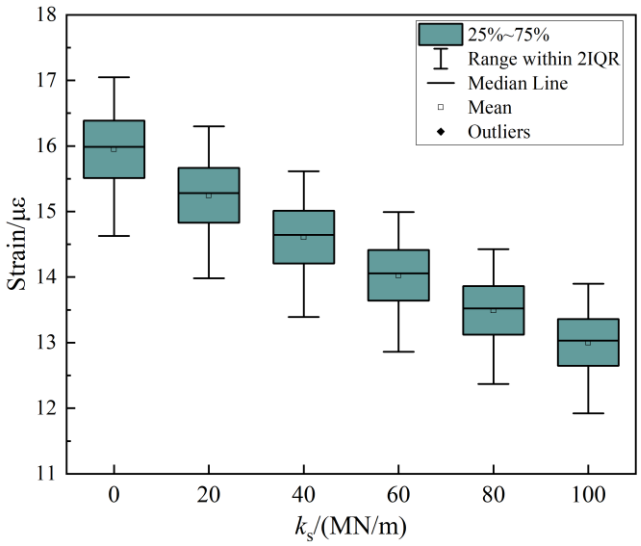

Figure 11. Strain boxplot of pavement under different shear stiffness.

The displacement response (**Figure 12**) follows a similar pattern. As the shear stiffness increases, the magnitude of the maximum displacement (in the negative direction) decreases. When shear stiffness increases from 0 MN/m to 100 MN/m, the

maximum displacement decreases from nearly −0.29 mm to −0.22 mm. Higher shear stiffness helps to reduce vertical deformation of the pavement surface, enhancing the geometric stability of the pavement. The boxplots (**Figure 13**) further demonstrate that increased shear stiffness reduces the range of displacement fluctuations, indicating that shear stiffness significantly improves the pavement's resistance to deformation.

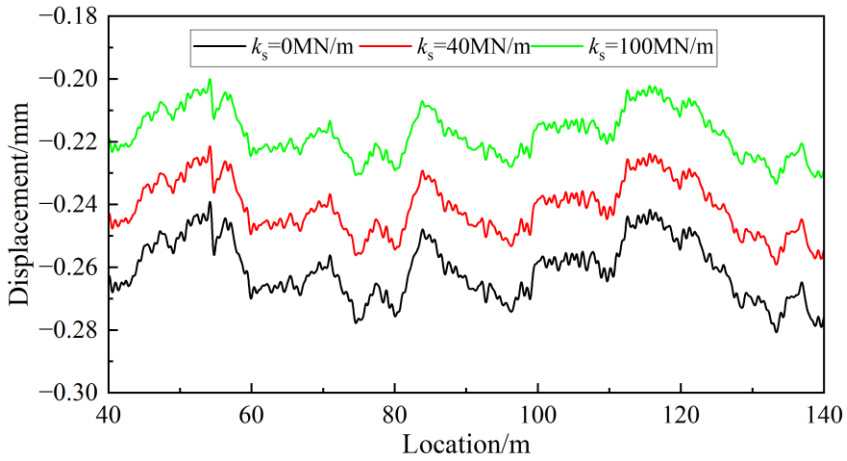

Figure 12. Pavement displacement under different shear stiffness.

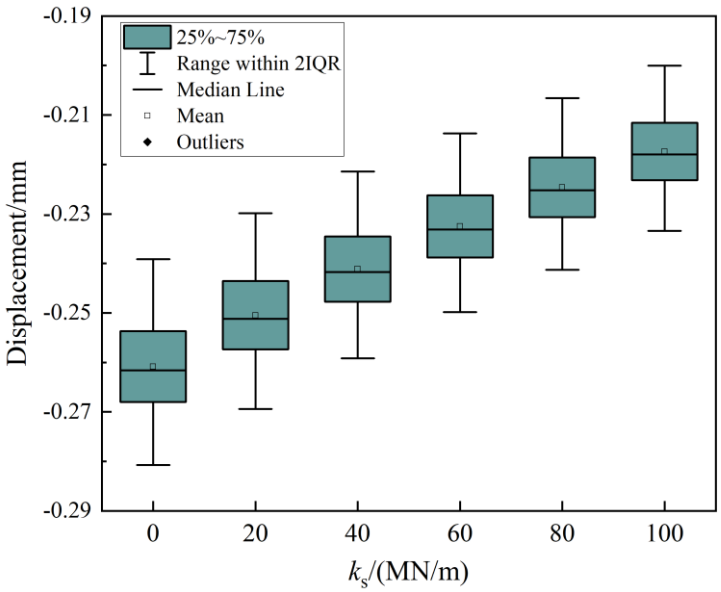

Figure 13. Displacement boxplot of pavement under different shear stiffness.

Although many traditional models did not consider the shear stiffness of the subgrade, the results of this study show that the lateral connectivity provided by the subgrade's shear stiffness significantly enhances the pavement's ability to resist external forces. Under the same dynamic load conditions, pavement structures with higher shear stiffness experience smaller dynamic strain and displacement. This contrasts with previous studies, such as those by Chen et al. [7] and Kim et al. [10], which comprehensively analyzed the dynamic response of pavement structures but did not account for the lateral support provided by subgrade shear stiffness. This study expands on their findings by demonstrating that models incorporating subgrade shear stiffness can more accurately predict pavement behavior under aircraft loads. The

Winkler model neglects the lateral interaction of the soil, underestimating the foundation's resistance to external forces, which results in relatively larger dynamic responses of the pavement structure and leads to a conservative design. Therefore, a foundation model that accounts for the subgrade shear stiffness should be adopted in pavement design, as it significantly enhances the durability and stability of the pavement structure. The research findings provide valuable insights for the revision and optimization of pavement design standards.

5.3. Effect of pavement structure on aircraft response

As shown in **Figure 14**, the analysis of various pavement structural parameters, including surface layer thickness, base layer thickness, base layer modulus, and shear stiffness, shows that these factors have minimal impact on the acceleration of the aircraft's center of gravity. Across all variations in these parameters, the mean and range of fluctuations in the aircraft's center of gravity acceleration remain largely unchanged, indicating that the pavement structure has a limited direct effect on the aircraft's dynamic response.

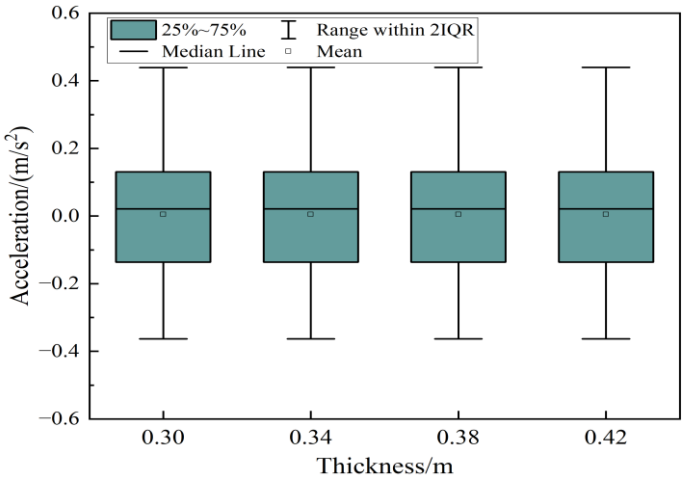

(a) surface layer thickness.

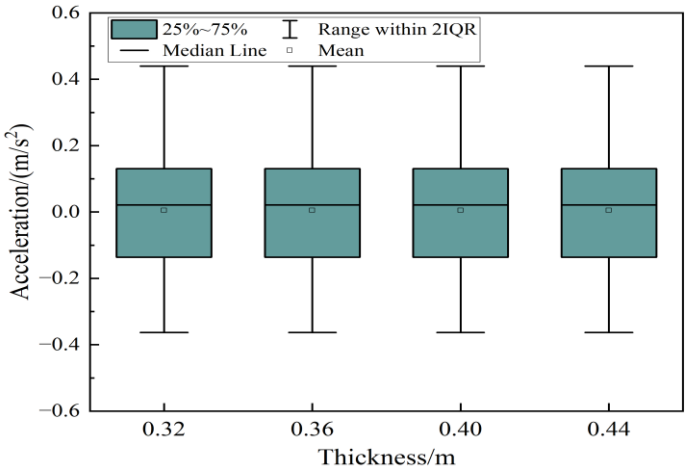

(b) base layer thickness.

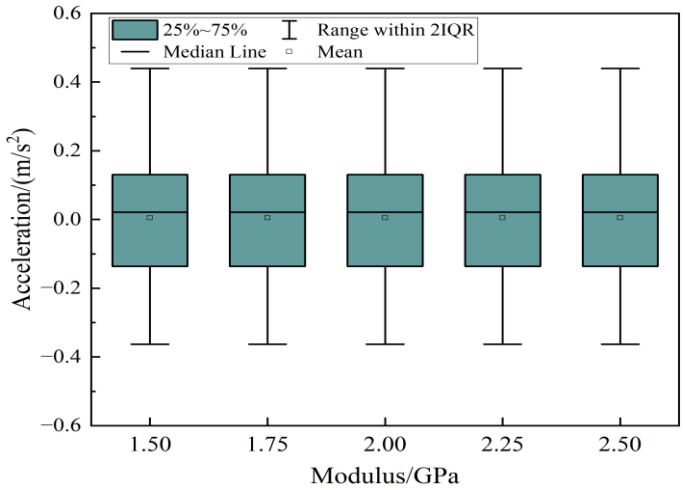

(c) base layer modulus.

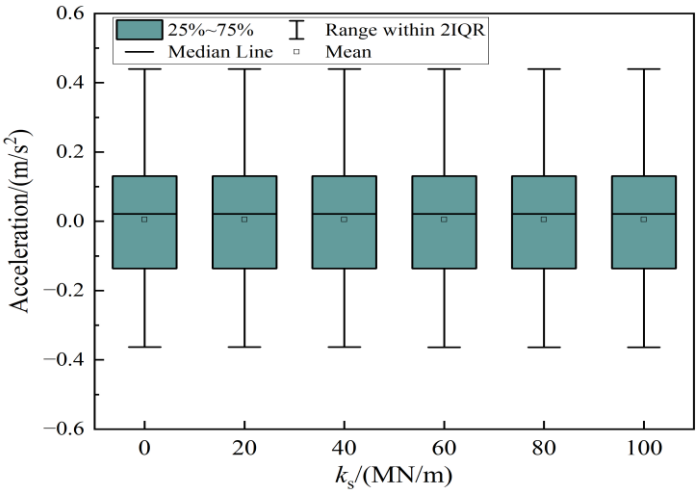

(d) subgrade shear stiffness.

Figure 14. Aircraft acceleration boxplot under pavement structure parameters.

This limited impact can be attributed to the combination of a rigid pavement and a semi-rigid base, which together create a highly stiff overall structure. This high stiffness allows the pavement to effectively resist deformation under external loads, resulting in minimal changes to the aircraft's center of gravity acceleration. While the thickness and modulus of the pavement play crucial roles in controlling the strain and displacement of the pavement itself, their influence on the dynamic response of the aircraft (such as its center of gravity acceleration) is relatively small.

In contrast, surface irregularities are more likely to have a significant impact on the aircraft's vibration response. Unevenness on the pavement surface directly affects the vibration and displacement of the aircraft during landing and taxiing, and this dynamic effect is often more pronounced than the influence of changes in pavement stiffness. Therefore, while pavement structural design is important for optimizing stress distribution and the long-term durability of the runway, its effect on the aircraft's center of gravity acceleration is relatively minor.

5.4. Influence of aircraft taxiing speed

This study analyzed the effect of different taxiing speeds on the dynamic response of the aircraft and runway system, focusing on the dynamic load coefficient of the right landing gear, the acceleration of the aircraft's center of gravity, the longitudinal dynamic strain at the bottom of the pavement surface, and pavement displacement. As shown in **Figure 15**, the results show that as the taxiing speed increases, the mean dynamic load coefficient decreases. This is because the lift generated by the aircraft is proportional to the square of the taxiing speed, and at higher speeds, the lift significantly reduces the dynamic load coefficient. Additionally, the range of fluctuation in the dynamic load coefficient increases with speed, indicating that the roughness of the runway surface has a stronger impact on the aircraft as speed increases. Notably, the maximum dynamic load coefficient occurs at a speed of 40 km/h, which is closely related to the interaction between taxiing speed and runway roughness.

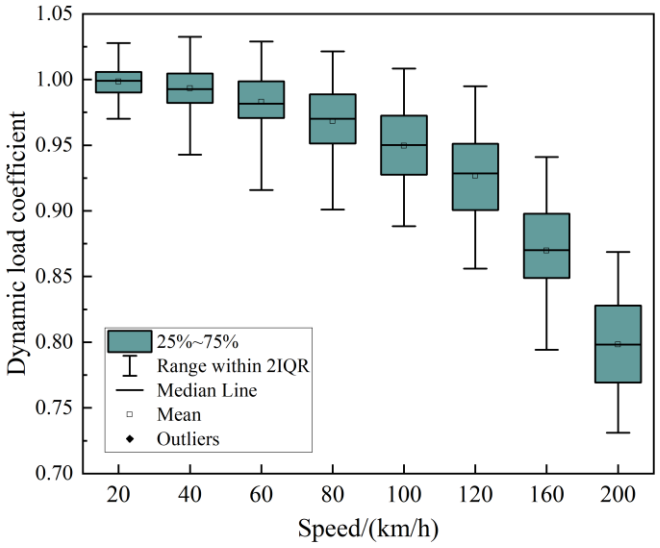

Figure 15. Aircraft dynamic load coefficient at different speeds.

It is important to note that the maximum value observed at 40 km/h is specific to the conditions of the fourth runway at Shanghai Pudong Airport, including the runway roughness and the type of aircraft used. Different airports and aircraft types may produce different maximum values, and as such, the conclusions of this study should be adjusted according to specific operational conditions.

As illustrated in **Figure 16**, the variation in the center of gravity acceleration follows a different pattern from the dynamic load coefficient. As taxiing speed increases, the fluctuation range of the center of gravity acceleration increases, indicating that the effect of runway roughness on aircraft vibration intensifies at higher speeds, while the lift has minimal impact on the center of gravity acceleration due to its relatively stable nature during taxiing.

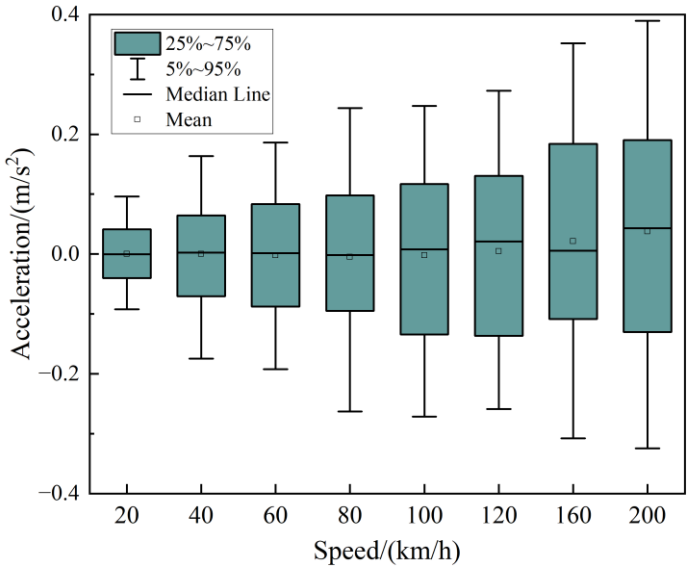

Figure 16. Acceleration of the center of gravity of the aircraft at different speeds.

The research results indicate that when evaluating runway smoothness and analyzing the structural forces on the aircraft, the most unfavorable aircraft speed should be used. If the control parameter is the aircraft's vibration and structural force condition, the most unfavorable speed should be the critical speed induced by the combined effects of aircraft lift and runway smoothness. If the control parameter is the aircraft's vibration acceleration, the most unfavorable speed can be taken as the maximum takeoff speed.

From **Figures 17** and **18**, it is evident that taxiing speed has a significant impact on the longitudinal dynamic strain at the bottom of the pavement surface. As the taxiing speed increases from 20 km/h to 200 km/h, the mean longitudinal dynamic strain decreases from 17.1 με to 13.8 με, a reduction of 19.3%. This numerical change indicates that at higher speeds, the overall strain experienced by the runway decreases. The physical explanation for this phenomenon is that as speed increases, the lift generated by the aircraft also increases, partially offsetting the vertical pressure on the runway, which leads to a reduction in dynamic strain.

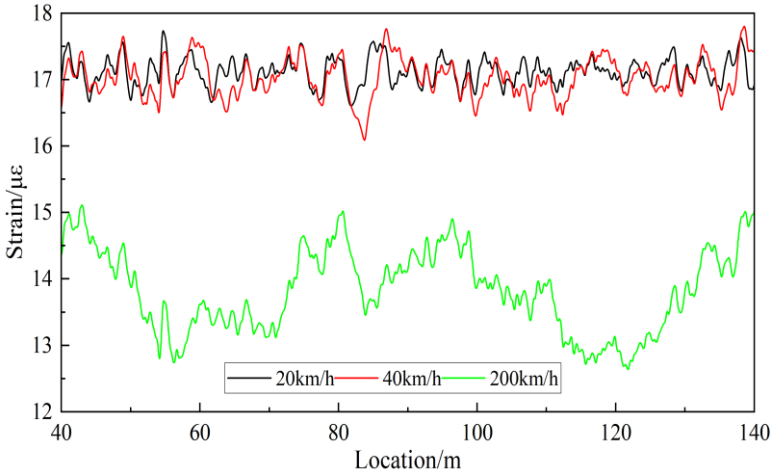

Figure 17. Longitudinal dynamic strain at surface bottom at different speeds.

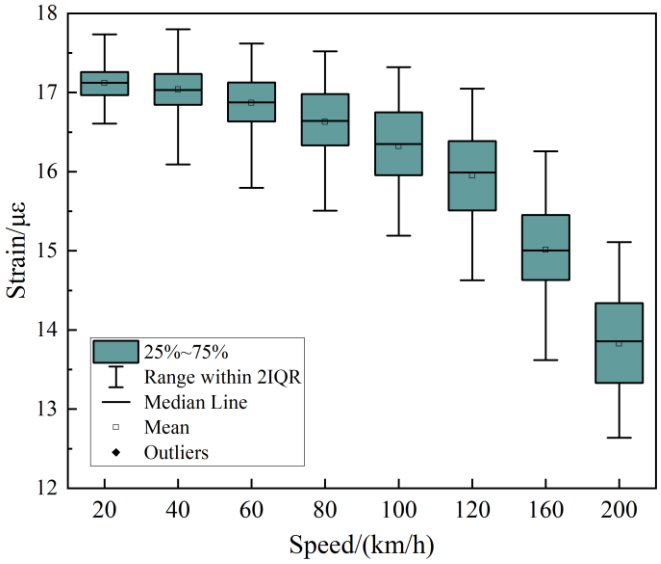

Figure 18. Dynamic strain boxplot of pavement at different speeds.

However, despite the decrease in the mean dynamic strain, the range of dynamic strain fluctuations significantly increases with speed. Specifically, as taxiing speed increases from 20 km/h to 200 km/h, the standard deviation of the dynamic strain rises from 0.21 με to 0.62 με, an increase of 195.2%. This indicates that at higher taxiing speeds, the roughness of the runway has a greater impact on local dynamic strain, leading to increased variability in strain. In other words, certain local areas of the runway experience greater stress due to the enhanced coupling effect between roughness excitation and the local properties of the runway at higher speeds.

Additionally, the maximum dynamic strain occurs at 40 km/h, reaching a peak of 17.8 με. This trend is consistent with the change in the dynamic load coefficient of the aircraft. At 40 km/h, the combination of roughness excitation and aircraft lift causes the dynamic strain to peak. At this speed, the effect of roughness excitation on the runway exceeds the effect of lift in reducing the dynamic load, resulting in the maximum strain. The research results suggest that in runway structural design, the aircraft's taxiing speed should be considered, and the maximum pavement structural response at the aircraft's critical speed should be used.

Compared to previous studies, such as the random vibration analysis of a coupled aircraft/runway system by Hou et al. [2] and the assessment of aircraft landing gear cumulative stroke for runway roughness evaluation by Liu et al. [20], this study reaches similar conclusions. Both studies show that the dynamic load coefficient and center of gravity acceleration exhibit similar trends as speed increases. However, this study provides a more comprehensive and systematic analysis by not only examining the dynamic responses at different taxiing speeds but also offering a detailed exploration of both aircraft and runway vibrations, yielding richer and more complete findings.

6. Conclusions

This research focuses on the dynamic interaction between aircraft and runways, emphasizing the critical role of the semi-rigid base in three-dimensional coupled vibrations. Numerical simulations based on the Pasternak foundation model, using data from Shanghai Pudong International Airport, examine how structural parameters influence load factors, strain, and displacement. The study provides valuable insights into optimizing runway design by highlighting the semi-rigid base's importance.

The results show that increasing the base layer modulus from 1.50 GPa to 2.50 GPa reduces maximum strain by 22.4%, from 16.5 με to 12.8 με. Similarly, increasing base thickness from 0.32 m to 0.44 m decreases strain by 17.8%. Enhancing subgrade shear stiffness from 0 MN/m to 100 MN/m further reduces strain from 17 με to 13 με. Additionally, as taxiing speed increases, the mean longitudinal strain decreases from 17.1 με to 13.8 με. These findings demonstrate that the supporting function of the semi-rigid base layer and the subgrade shear stiffness are crucial in reducing the structural response of the runway, thereby improving its durability and enhancing aircraft safety. During the aircraft's taxiing process, there are two critical speeds that significantly influence the dynamic response of both the aircraft and the runway. In structural design and evaluation, particular attention should be paid to the semi-rigid base layer, subgrade shear stiffness, and aircraft taxiing speed. Neglecting these factors may result in inaccurate assessments of runway performance.

The study is limited by focusing on a single aircraft type and airport conditions. Future work should explore various aircraft models and environmental conditions to generalize these findings. In practical scenarios, the impact of an aircraft on the runway is oblique. This paper only considers the vertical forces exerted by the aircraft's landing gear on the runway. Further research on oblique forces and the use of a new structure-preserving method in the aircraft-runway coupled model will be conducted in future studies.

Author contributions: Conception and design, SL, JL and TH; data collection, WM; analysis and interpretation of results, SL, JL and TH; writing—original draft preparation, JL and TH. All authors have read and agreed to the published version of the manuscript.

Funding: This research was funded by the Natural Science Foundation of Shanghai (grant number 23ZR1466300) and the National Natural Science Foundation of China (grant number 52402430).

Acknowledgments: The authors would like to acknowledge the administrative and technical assistance provided by the Key Laboratory of Road and Traffic Engineering, Ministry of Education, Tongji University. We would also like to thank the Shanghai Pudong International Airport authorities for providing essential data and access to the runway. Special thanks are extended to the lab team at Tongji University for their contributions to equipment setup and data collection.

Availability of data and materials: The data that support the findings of this study are available from the corresponding author, [T.H.], upon reasonable request.

Conflict of interest: The authors declare no conflict of interest.

References

1. Hu G, Li P, Xia H, et al. Study of the Dynamic Response of a Rigid Runway with Different Void States during Aircraft Taxiing. Applied Sciences. 2022; 12(15): 7465. doi: 10.3390/app12157465
2. Hou T, Liu S, Ling J, et al. Vibration Response Law of Aircraft Taxiing under Random Roughness Excitation. Applied Sciences. 2023; 13(13): 7386. doi: 10.3390/app13137386
3. Nita P. Dynamic interaction of military aircraft working on a cement concrete airfield pavement. Transportation Overview - Przegląd Komunikacyjny. 2020; 2020(2): 37-45.
4. Liu C, Chong X, Wang L, et al. Numerical Analysis on the Mechanical Properties of the Concrete Precast Pavement of Runways under the Wheel Load. Applied Sciences. 2022; 12(19): 9826. doi: 10.3390/app12199826
5. Liu S, Ling J, Tian Y, et al. Random Vibration Analysis of a Coupled Aircraft/Runway Modeled System for Runway Evaluation. Sustainability. 2022; 14(5): 2815. doi: 10.3390/su14052815
6. Li S, Guo J. Modeling and Dynamic Analysis of an Aircraft–Pavement Coupled System. Journal of Vibration Engineering & Technologies. 2022; 11(7): 3507-3519. doi: 10.1007/s42417-022-00764-w
7. Chen HY, Ding H, Chen LQ. Coupling Vibration of a Moving Oscillator with a Sandwich Plate on Nonlinear Foundations. Journal of Vibration Engineering & Technologies. 2024. doi: 10.1007/s42417-024-01315-1
8. Liu S, Tian Y, Yang G, et al. Effect of space for runway roughness evaluation. International Journal of Pavement Engineering. 2022; 24(2). doi: 10.1080/10298436.2022.2141739
9. Sawant V. Dynamic analysis of rigid pavement with vehicle–pavement interaction. International Journal of Pavement Engineering. 2009; 10(1): 63-72. doi: 10.1080/10298430802342716
10. Kim SM, Won MC, McCullough BF. Airport pavement response under moving dynamic aircraft loads. In Designing, Constructing, Maintaining, and Financing Today's Airport Projects. 2002; 1-10.
11. Patil VA, Sawant VA, Deb K. 2-D finite element analysis of rigid pavement considering dynamic vehicle–pavement interaction effects. Applied Mathematical Modelling. 2013; 37(3): 1282-1294. doi: 10.1016/j.apm.2012.03.034
12. Yang S, Li S, Lu Y. Investigation on dynamical interaction between a heavy vehicle and road pavement. Vehicle System Dynamics. 2010; 48(8): 923-944. doi: 10.1080/00423110903243166
13. Belabed Z, Tounsi A, Bousahla AA, et al. Accurate free and forced vibration behavior prediction of functionally graded sandwich beams with variable cross-section: A finite element assessment. Mechanics Based Design of Structures and Machines. 2024: 1-34. doi: 10.1080/15397734.2024.2337914
14. Belabed Z, Tounsi A, Bousahla AA, et al. Free vibration analysis of Bi-Directional Functionally Graded Beams using a simple and efficient finite element model. Structural Engineering and Mechanics, 2024; 90(3): 233-252.
15. Attia A, Berrabah AT, Bourada F, et al. Free Vibration Analysis of Thick Laminated Composite Shells Using Analytical and Finite Element Method. Journal of Vibration Engineering & Technologies. 2024. doi: 10.1007/s42417-024-01322-2
16. Lakhdar Z, Chorfi SM, Belalia SA, et al. Free vibration and bending analysis of porous bi-directional FGM sandwich shell using a TSDT p-version finite element method. Acta Mechanica. 2024; 235(6): 3657-3686. doi: 10.1007/s00707-024-03909-y
17. Hu W, Xu M, Zhang F, et al. Dynamic analysis on flexible hub-beam with step-variable cross-section. Mechanical Systems and Signal Processing. 2022; 180: 109423. doi: 10.1016/j.ymssp.2022.109423
18. Hu W, Xi X, Song Z, et al. Coupling dynamic behaviors of axially moving cracked cantilevered beam subjected to transverse

harmonic load. Mechanical Systems and Signal Processing. 2023; 204: 110757. doi: 10.1016/j.ymssp.2023.110757

19. Hu W, Zhou Y, Liu Q, et al. Vibrational analysis of finite plate on elastic foundation subjected to oblique impact. Journal of Mechanics of Materials and Structures. 2024; 19(3): 419-433. doi: 10.2140/jomms.2024.19.419
20. Liu S, Ling J, Tian Y, et al. Assessment of aircraft landing gear cumulative stroke to develop a new runway roughness evaluation index. International Journal of Pavement Engineering. 2021; 23(10): 3609-3620. doi: 10.1080/10298436.2021.1910823